Vietnam Journal of Science and Technology ***57*** *(2) (2019) 198-206*
doi:10.15625/2525-2518/57/2/13071

LAYERED O3-$NaFe_{0.5}Co_{0.5}O_2$ AS HIGH CAPACITY AND LOW- COST MATERIAL FOR SODIUM ION BATTERIES

Nguyen Van Hoang[1, *], Mai Ngoc Phuoc[1], Huynh Le Thanh Nguyen[2], Nguyen Dinh Quan[3], Tran Van Man[1, 2], Le My Loan Phung[1, 2]

[1]*Faculty of Chemistry, University of Science, VNU-HCMC, 227 Nguyen Van Cu St., Dist. 5, Ho Chi Minh City*

[2]*Applied Physical Chemistry Laboratory, Faculty of Chemistry, University of Science, VNU-HCMC, 227 Nguyen Van Cu St., Dist. 5, Ho Chi Minh City*

[3]*Laboratory of Biofuel and Biomass Research, Research Institute for Sustainable Energy, University of Technology, VNU-HCMC, 227 Nguyen Van Cu St., Dist. 5, Ho Chi Minh City*

[*]Email: *nvhoang@hcmus.edu.vn*

Received: 4 September 2018; Accepted for publication: 23 November 2018

Abstract. In this work, O3-$NaFe_{0.5}Co_{0.5}O_2$ layered cathode material was synthesized by solid state reaction at 900 ^oC followed by a quenching step at 600 ^oC in argon atmosphere. X-rays diffraction patterns indicated that O3-layered structure could be maintained after a quenching process at 600 ^oC. The chemical composition and morphology of the synthesized material were analyzed by Atomic Absorption Spectroscopy (AAS) and Scanning Electron Microscopy (SEM). The electrochemical properties were evaluated by Cyclic Voltammetry (CV) and charge-discharge cycling. The material $NaFe_{0.5}Co_{0.5}O_2$ shows the sloped discharge curves with high flat voltage plateau and excellent cycling stability. The reversible capacity of about 120 mAh/g at rate C/10 and good capacity retention after 100 cycles were obtained. The rate capability of material was investigated at the current density up to 2 C in voltage range 2.5-4 V.

Keywords: O3-layered oxide, $NaFe_{0.5}Co_{0.5}O_2$, high capacity, sodium ion batteries.

Classification numbers: 2, 3.

1. INTRODUCTION

In the last and coming decades, Li-ion batteries (LIB) are still the best of choice power sources for electronic devices and electric vehicles due to its high voltage, light weight, high energy power and long cycle life which are well-adapted to the user requirements. However, it should be noted that the Li-ion cell price is relatively expensive and keeps on increasing due to lithium resource limitation [1]. As a result, the big challenges for large scale application of lithium batteries are encountered in near future.

Recently, the research of Na-ion batteries (NIB) as a next generation beyond LIB has been increased significantly [2–8]. The use of sodium metal in batteries has been explored for a long

time but stopped for a while due to the high rate development of LIB. The replacement of lithium by sodium as electrochemical carrier in Na-ion offers many benefits such as: cost reduce and bypass the concern about raw materials lacking. Some sodium-based electrode materials exhibited high performance in half-cell, as good as the lithium analogues, demonstrated that Na-ion batteries will be potentially replaced Li-ion batteries in most large-scale applications.

Layered $LiCoO_2$ was a pioneer cathode material used in commercial LIB since 1992 due to high power density, thus the researches in layered $NaCoO_2$ are relatively attracted [9,10]. However, the use of cobalt element must be reduced because of its harmful effect on the environment. Co could be replaced by other benign elements such as Ni, Mn, Fe, Ti etc. in P2 or O3-type based binary, ternary cathode materials [11–17]. They are two types of layered structure of alkaline transition metal oxides as Delmas et al. classified [18], therein, sodium ions are octahedral or trigonal-prismatic coordination on O3 and P2 type, respectively. The use of Fe is highly appreciated because of the environmental friendliness, structural stability and high redox potential. In addition, $NaFeO_2$ is a typical O3-layered oxide that should be well compatible with O3-$NaCoO_2$ phase. The ferrous content should be optimized to replace a high amount of cobalt in O3-$NaCoO_2$ phase. Thus, $NaFe_{0.5}Co_{0.5}O_2$ as a substituted phase showed the good performance combining of high capacity ($NaCoO_2$ phase) and high redox potential ($NaFeO_2$ phase) [12]. However, the electrochemical properties of the material were affected by synthesis condition which was finished by a quenching step from the calcination temperature (900 ^oC) [19]. The high quenching temperature made it difficult to handle, so it is probably practical interesting in lower the temperature.

In this work, the electrode material $NaFe_{0.5}Co_{0.5}O_2$ was synthesized with a quenching step occurred in argon atmosphere at lower temperature of 600 ^oC. The electrochemical tests showed that the sample exhibited a good structure stability with high capacity retention after 100 cycles and high discharge rate up to 2C in voltage 2.5-4.0 V.

2. MATERIALS AND METHODS

All the chemical reagents were purchased from Sigma-Aldrich and Merck with high purity (> 99 %). To prepare the $NaFe_{0.5}Co_{0.5}O_2$, the Na_2CO_3, $FeC_2O_4.H_2O$ and $Co(NO_3)_2.6H_2O$ precursors at a molar ratio of 1.05:0.5:0.5 (5% sodium excess) were firstly mixed in an alumina crucible, heated at 300 ^oC for 12 hours then the mixture was grinded to powder. The powder was then treated in two different conditions *(i)* using pressure 10,000 N/cm^2 to make the pellets and *(ii)* without pressure which were denoted as NFC-1 and NFC-2, respectively. The two samples (pelleted and non-pelleted) were calcinated at 900 ^oC for 12 hours. When the calcination finished and the oven's temperature lowered to 600 ^oC, the samples were transferred to glovebox filled with argon for quenching.

The material $NaFeO_2$ (NFO) and $NaCoO_2$ (NCO) was also synthesized in the same condition of NFC-1, but differed from the final calcination temperature 600 ^oC (NFO) and 800 ^oC (NCO).

The structure was analyzed by X-ray diffraction on a D8 Advance (Bruker) using CuKα radiation (λ = 1.5418 Å) with a scan rate of 0.02^o/step. SEM images of samples were collected on FE-SEM SU8100 equipment (Hitachi). Chemical composition was analyzed by Inductively coupled plasma atomic emission spectroscopy (ICP-AES, Perkin Elmer).

Electrochemical properties of materials were evaluated using Swagelok type cell with the cathode consists of 75 % active material, 20 % TIMCAL carbon black C65 and 5 % PTFE. The

cathode paste was laminated into thin film and cut into 10 mm diameters then dried in vacuum at 80 ^{o}C for at least 15 hours. A sodium slice was used as anode. The electrolyte was $NaClO_4$ 1 M in propylene carbonate (PC) with 2 % fluoroethylene carbonate (FEC) as additive. The half-cell was assembled in the glovebox filled with argon to avoid oxygen and moisture contact. The electrochemical performance of half-cell was tested on MPG-2 battery tester (Bio-logic) using galvanostatic charge-discharge at constant current in C/N rate (1C = 240 mAh/g) and Cyclic voltammetry method (CV) in rate of 0.1 mV/s.

3. RESULTS AND DISCUSSION

Figure 1 presents XRD patterns of mono and binary metal oxides. The diffraction patterns of NFO and NFC-1 indicated that the synthesized samples have an O3-type layered structure as α-$NaFeO_2$ with rhombohedral symmetry and R-3m space group (PDF#01-070-2030). The peak shifting to high theta degree (2θ) could be seen when replacing Fe^{3+} by smaller Co^{3+} in NFC samples, as a result, the lattice parameters of unit cell decreased respectively to strengthen the crystal structure [20]. Lattice parameters were calculated using CELREF software (version 3.0) and given in Table 1.

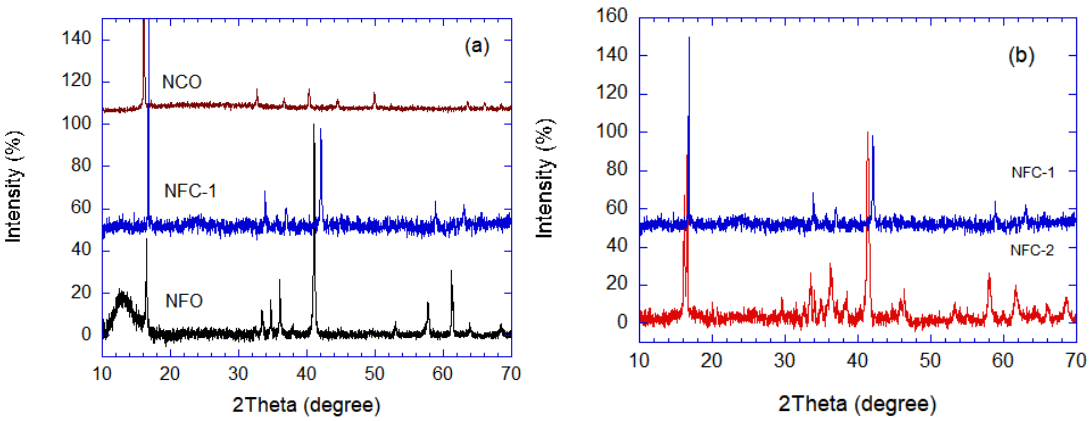

Figure 1. XRD patterns of pristine and substituted samples (a) and the NFC samples (b).

Table 1. Lattice parameters of synthesized samples.

Sample code	a (Å)	b (Å)	c (Å)	V (Å^3)
NFO	3.0166	3.0166	16.0580	126.55
NFC-1	2.9497	2.9497	15.8901	119.73
NCO	2.8294	2.8294	10.9386	75.84

The two lattice parameters a and c were reduced which could be reflected in shortening of M–O bonds length in layers and the distance between layers. XRD diffraction results indicated that the NCO sample did not get O3 phase at high temperature annealing, eventually P2 phase with hexagonal symmetry could be obtained ($Na_{0.74}CoO_2$, PDF#01-087-0274). Otherwise, the substituted NFC-1 exhibited O3-$NaFeO_2$ phase at low synthesis temperature of 600 ^{o}C [21-24]

and at high annealing condition of 900 ^oC. Thus, it proves the presence of Co^{3+} stabilized the O3-$NaFeO_2$ structure. XRD patterns of NFC-2 sample (without making pellet, Figure 1b) shows the presence of P2-Na_xCoO_2 and might be O3-$NaFe_{0.5}Co_{0.5}O_2$ because O3-$NaFeO_2$ could not stable at high temperature. This is possible resulted from poor contact of particles, so pelleting is referred to increase yield of synthesis.

The morphology was evaluated by SEM images (Figure 2). In the two samples, the particles exhibited undefined shape and the grain size distributed in range 2-3 µm with unexpected agglomeration.

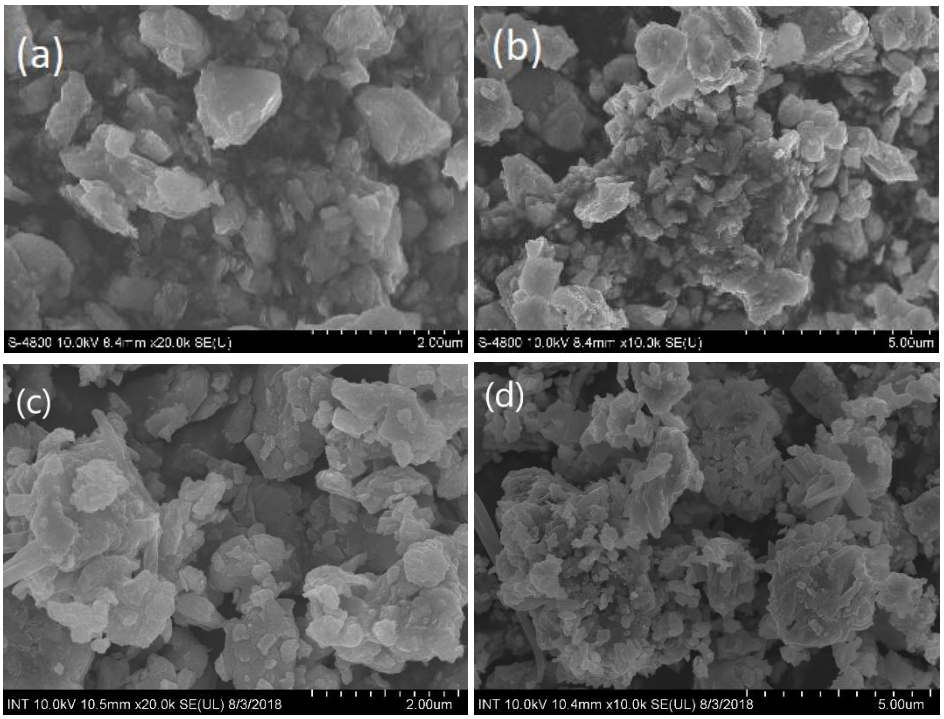

Figure 2. SEM images of (a-b) NFC-2 and (c-d) NFC-1.

The chemical composition of NFC-1 and NFC-2 determined by ICP-AES were $Na_{1.022}Co_{0.534}Fe_{0.466}O_{2.651}$, $Na_{0.960}Co_{0.576}Fe_{0.424}O_{2.909}$, respectively. The ratio of metallic elements is expectedly fitted to theoretical calculation, excepted for the concentration of oxygen. It means that the oxygen ratio in the sample is not only the real oxygen but might also include from moisture in air.

Figure 3 gives the comparison in electrochemical properties between two samples. Firstly, on CV curves, the sample NFC-1 shows the sharp and high intensity peaks (Figure 3b). On the forward scan, 4 anode peaks at potential of 3.1 V, 3.3 V, 3.6 V and 3.8 V indicated phase transfer during the extraction of sodium ion. On the backward scan, however, only two peaks at low potential were observed clearly. NFC-2 sample (without making pellet) displayed similarly the electrochemical active as NFC-1, but these peaks are broad with low intensity (Figure 3a). Additionally, small peaks (marked as ▼) could be the oxidation/reduction of impurity phase in NFC-2 sample.

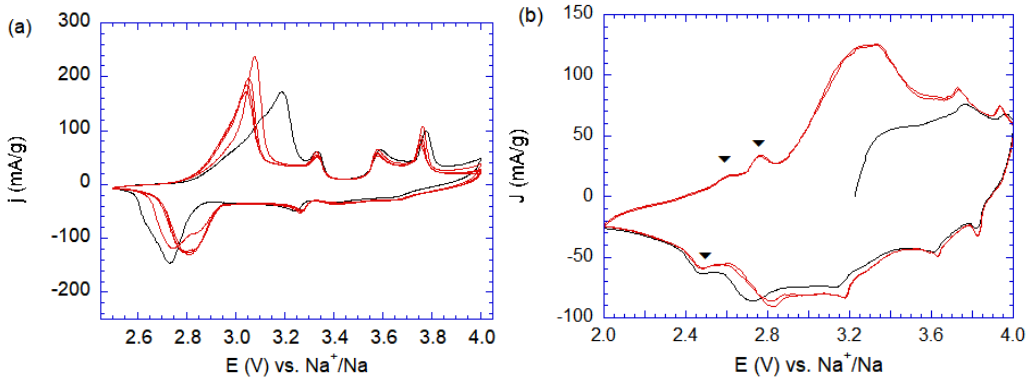

Figure 3. Cyclic voltammogram at scan rate 0.1 mV/s of NFC-1 (a) and NFC-2 (b).

Figure 4 and Figure 5 show the charge-discharge profiles of NFC-1, NFC-2 and the comparison with NCO and NFO materials.

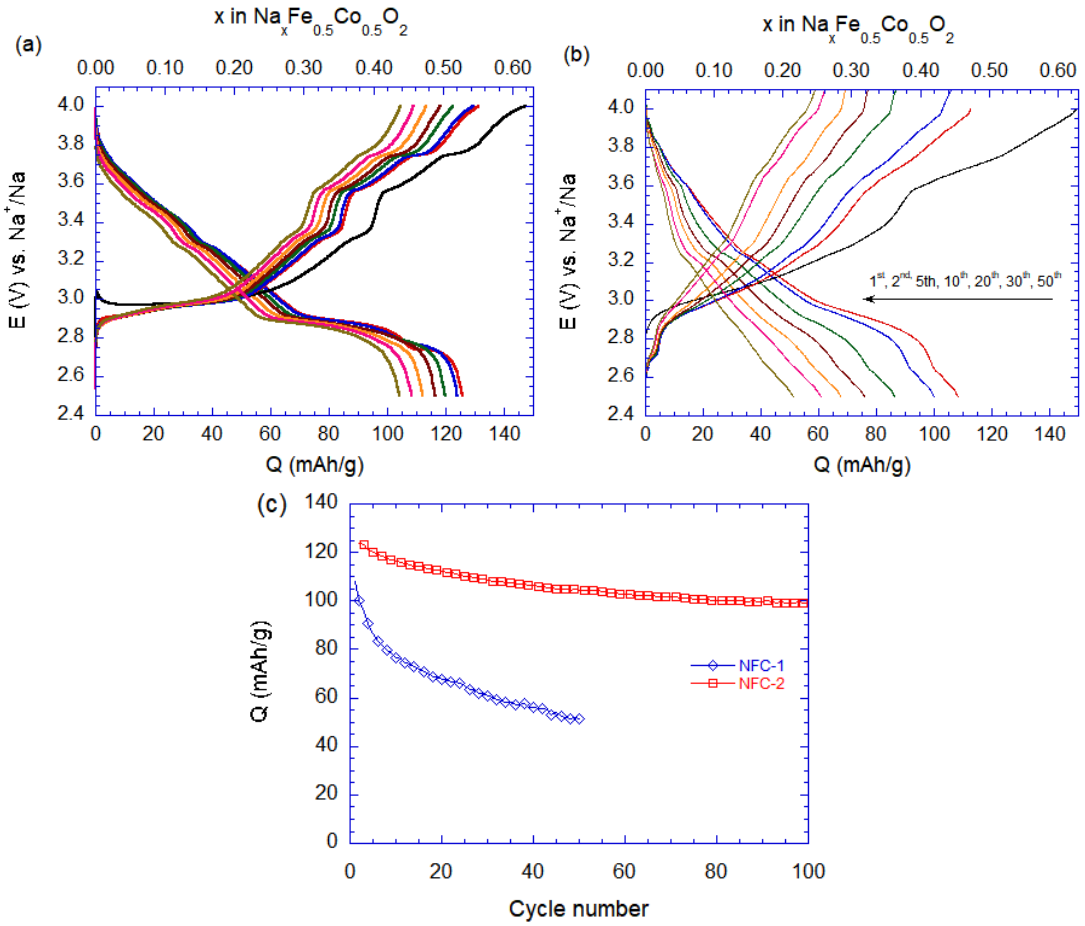

Figure 4. Cycling test of NFC-1 and NFC-2 samples at C/10 rate (a,b) and their specific capacity during the time (c).

On the charge-discharge curve of NFC samples (Figure 4a, b), the oxidation of Fe^{3+} to Fe^{4+} occurred at 2.9 V and the oxidation of Co^{3+} to Co^{4+} could be seen clearly within many voltage steps. On the discharge curve, the material exhibited a sloped curve and a relative flat plateaus at voltage 2.8 V. This profile is not due to the irreversible of phase transfer at low Na^+ content in charge and discharge process, but the remarkable reduce in propulsion between sodium and layere oxides at low sodium content [25]. The capacity of the flat plateau region and the high voltage region (including the slope and the voltage step region) is almost the same, which is consistent with the Fe^{3+}/Co^{3+} ratio about unity. The voltage-capacity profile of NFC-1 and NFC-2 are similar, however the capacity of NFC-2 faded dramatically after 50 cycles. The charge-discharge curves of NFC-2 are relatively smooth, but the plateau not pronounced. The voltage step at 3.2 V pronounced after several cycles instead, and the charge-discharge curve is rather similar to that of Na_xCoO_2 (Figure 5). It could be suggested a phase decomposition of $Na_xFe_{0.5}Co_{0.5}O_2$ into Na_xCoO_2 and Na_xFeO_2 phase during the cycling process, accompanied with the decrease in capacity.

The capacity retention after 50th of NFC-2 is 46.3 % while NFC-1 shows a stable cycling with about 80 % capacity retention after 100 cycles (Figure 4c).

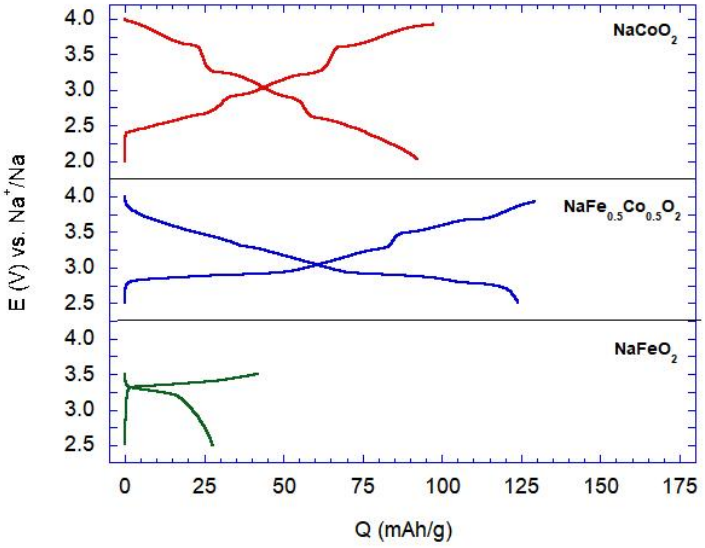

Figure 5. Typical charge-discharge curve of different samples NCO, NFC-1 and NFO.

In Figure 5, NCO gives a capacity of ca. 90 mAh/g in potential range 2-4 V with stepwise voltage profile due to multiple reversible phase transitions. In contrast, NFO exhibited a low capacity ca. 25 mAh/g in potential range 2.5-3.4 V with nearly flat voltage profile. NFC sample as a solid solution of NCO and NFO, a merged voltage profile could be seen with a flat plateau and multi voltage steps at low and higher voltage region, respectively. NFC could stabilize the Fe^{4+}/Fe^{3+} in the structure and increase inversible capacity in comparing to NCO and NFO samples. NFC exhibited a capacity of ca. 125 mAh/g in voltage range 2.5-4 V. This result was in well agreement with previous study, Fe-substitution in $NaCoO_2$ could enhance the performance of material [12, 25].

Figure 6 shows the results of NFC-1 cycled at different rates from C/10 to 2 C for capability performance. The material shows very good cycling stability and high rate capability. In the voltage range of 2.5-4 V, the average reversible capacity obtained at C/10, C/5, C/2, 1 C

and 2 C is 133 mAh/g, 125 mAh/g, 115 mAh/g, 105 mAh/g and 88.5 mAh/g, respectively. When the current density returns to C/5 at 50th cycle, the average capacity is 123 mAh/g, slightly less than the initial value of 125 mAh/g. Moreover, the NFC could be cycled at very high rate 30C but only at the lower cutoff voltage 1.5 V, this ability is promising application for the high-rate capacity Na-intercalation material [12].

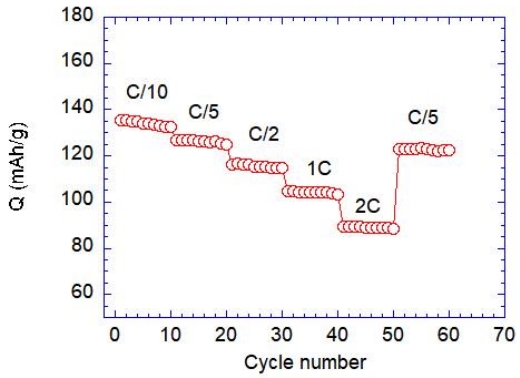

Figure 6. Rate capability test of NFC-1 cathode material.

Following the upper part on structure stability, X-ray diffraction was conducted in cathode film of samples at cutoff potential 2 V after 20 discharge-charge cycles, the results was seen in Figure 7. At this discharge state, the materials should be returned to their original structures. The similarity between the XRD pattern of pristine NFC-1 and the one after cycling exhibits high structure stability of the sample. While, only two high intensity peaks of P2-Na_xCoO_2 could be seen clearly in the pattern of NFC-2 film. This coincided with above noticed thing about the change in voltage-profile of the samples after several continuous cycling.

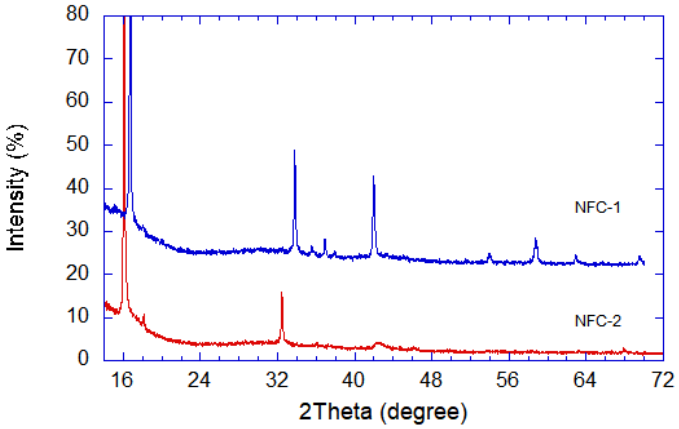

Figure 7. XRD patterns of cathode films at cutoff potential 2 V after 20 charge-discharge cycles.

4. CONCLUSIONS

O3-$NaFe_{0.5}Co_{0.5}O_2$ material was successfully synthesized at 900 ^oC following a quenching step at 600 ^oC in argon environment. The pelleted sample NFC-1 shows the promising electrochemical properties with a slope and long discharge plateau resulting in redox couple Co^{4+}/Co^{3+} and Fe^{4+}/Fe^{3+} at high and lower voltage region, respectively. The material delivers

high capacity and high rate capability with discharge rate up to 2 C in voltage range 2.5 – 4 V. However, due to structure sensitivity, the synthesized materials must be stored in dry or inert air to prolong electrochemical properties.

Acknowledgements. This research is funded by University of Science, VNU-HCM, under grant number T2018-10.

REFERENCES

1. Nitta N., Wu F., Lee J.T., Yushin G. - Li-ion battery materials: present and future, Mater. Today **18** (2015) 252-264.
2. Mahlia T. M. I, Saktisahdan T. J., Jannifar A., Hasan M. H., Matseelar H. S. C. - A review of available methods and development on energy storage; technology update, Renew. Sustain. Energy Rev. **33** (2014) 532-545.
3. Yabuuchi N., Kubota K., Dahbi M., Komaba S. - Research Development on Sodium-Ion Batteries, Chem. Rev. **114** (2014) 11636-11682.
4. Ortiz-Vitoriano N., Drewett N. E., Gonzalo E., Rojo T. - High performance manganese-based layered oxide cathodes: overcoming the challenges of sodium ion batteries, Energy Env. Sci. **10** (2017) 1051-1074.
5. Liu Y., Liu X., Wang T., Fan L.-Z., Jiao L. - Research and application progress on key materials for sodium-ion batteries, Sustain. Energy Fuels **1** (2017) 986-1006.
6. Wang L.P., Yu L., Wang X., Srinivasan M., Xu Z.J. - Recent developments in electrode materials for sodium-ion batteries, J Mater Chem A **3** (2015) 9353-9378.
7. Massé R. C., Uchaker E., Cao G. - Beyond Li-ion: electrode materials for sodium- and magnesium-ion batteries, Sci. China Mater. **58** (2015) 715-766.
8. Pan H., Hu Y.-S., Chen L. - Room-temperature stationary sodium-ion batteries for large-scale electric energy storage, Energy Environ. Sci. **6** (2013) 2338.
9. Rami Reddy B. V., Ravikumar R., Nithya C., Gopukumar S. - High performance Na_xCoO_2 as a cathode material for rechargeable sodium batteries, J. Mater. Chem. A **3** (2015) 18059-18063.
10. Ding J. J., Zhou Y. N., Sun Q., Yu X. Q., Yang X. Q., Fu Z. W. - Electrochemical properties of P2-phase $Na_{0.74}CoO_2$ compounds as cathode material for rechargeable sodium-ion batteries, Electrochimica Acta **87** (2013) 388-393.
11. Yang P., Zhang C., Li M., Yang X., Wang C., Bie X., Wei Y., Chen G., Du F. - P2-$NaCo_{0.5}Mn_{0.5}O_2$ as a Positive Electrode Material for Sodium-Ion Batteries, Chem Phys Chem. **16** (2015) 3408-3412.
12. Yoshida H., Yabuuchi N., Komaba S. - $NaFe_{0.5}Co_{0.5}O_2$ as high energy and power positive electrode for Na-ion batteries, Electrochem. Commun. **34** (2013) 60-63.
13. Li X., Wu D., Zhou Y.N., Liu L., Yang X.-Q., Ceder G. - O3-type $Na(Mn_{0.25}Fe_{0.25}Co_{0.25}Ni_{0.25})O_2$: A quaternary layered cathode compound for rechargeable Na ion batteries, Electrochem. Commun. **49** (2014) 51-54.
14. Sathiya M., Hemalatha K., Ramesha K., Tarascon J.-M., Prakash A.S. - Synthesis, Structure, and Electrochemical Properties of the Layered Sodium Insertion Cathode Material: $NaNi_{1/3}Mn_{1/3}Co_{1/3}O_2$, Chem. Mater. **24** (2012) 1846-1853.

15. Nguyen V. H., Nguyen T. T. L., Huynh L. T. N., Le M. L. P., Tran V. M. - Electrochemical properties of sol-gel $NaNi_{1/3}Mn_{1/3}Co_{1/3}O_2$ cathode material, J. Chemistry **55** (2017) 105-109.
16. Doubaji S., Ma L., Asfaw H. D., Izanzar I., Xu R., Alami J., Lu J., Wu T., Amine K., Edström K., Saadoune I. - On the P2-$Na_xCo_{1-y}(Mn_{2/3}Ni_{1/3})_yO_2$ Cathode Materials for Sodium-Ion Batteries: Synthesis, Electrochemical Performance, and Redox Processes Occurring during the Electrochemical Cycling, ACS Appl. Mater. Interfaces **10** (2018) 488-501.
17. Wang H., Liao X. Z., Yang Y., Yan X., He Y. S., Ma Z. F. - Large-Scale Synthesis of $NaNi_{1/3}Fe_{1/3}Mn_{1/3}O_2$ as High Performance Cathode Materials for Sodium Ion Batteries, J. Electrochem. Soc. **163** (2016) A565-A570.
18. Delmas C., Fouassier C., Hagenmuller P. - Structural classification and properties of the layered oxides, Physica **99B** (1980) 81-85.
19. Amaha K., Kobayashi W., Akama S., Mitsuishi K., Moritomo Y. - Interrelation between inhomogeneity and cyclability in O3-$NaFe_{1/2}Co_{1/2}O_2$, Phys. Status Solidi RRL - Rapid Res. Lett. **11** (2017) 1600284.
20. Viciu L., Bos J. W. G., Zandbergen H. W., Huang Q., Foo M. L., Ishiwata S., Ramirez A. P., Lee M., Ong N. P., Cava R. J. - Crystal structure and elementary properties of Na_xCoO_2 (x = 0.32, 0.51, 0.6, 0.75, and 0.92) in the three-layer $NaCoO_2$ family, Phys. Rev. B **73** (2006) 174104.
21. Monyoncho E., Bissessur R. - Unique properties of α-$NaFeO_2$: De-intercalation of sodium via hydrolysis and the intercalation of guest molecules into the extract solution, Mater. Res. Bull. **48** (2013) 2678-2686.
22. Kikkawa S., Miyazaki S., Koizumi M. - Sodium deintercalation from α-$NaFeO_2$, Mater. Res. Bull. **20** (1985) 373-377.
23. Zhao J., Zhao L., Dimov N., Okada S., Nishida T. - Electrochemical and Thermal Properties of α-$NaFeO_2$ Cathode for Na-Ion Batteries, J. Electrochem. Soc. **160** (2013) A3077-A3081.
24. Viret M., Rubi D., Colson D., Lebeugle D., Forget A., Bonville P., Dhalenne G., Saint-Martin R., André G., Ott F. - β-$NaFeO_2$, a new room-temperature multiferroic material, Mater. Res. Bull. **47** (2012) 2294-2298.
25. Kubota K., Asari T., Yoshida H., Yaabuuchi N., Shiiba H., Nakayama M., Komaba S. - Understanding the Structural Evolution and Redox Mechanism of a $NaFeO_2$-$NaCoO_2$ Solid Solution for Sodium-Ion Batteries, Adv. Funct. Mater. **26** (2016) 6047-6059.